eprints@whiterose.ac.uk
https://eprints.whiterose.ac.uk/

# Low Excess Noise of Al$_{0.85}$Ga$_{0.15}$As$_{0.56}$Sb$_{0.44}$ Avalanche Photodiode from Pure Electron Injection

Jonathan Taylor-Mew, Vladimir Shulyak, Benjamin White, Chee Hing Tan, *Senior Member, IEEE*, and Jo Shien Ng*, Member, IEEE*

*Abstract*— **Avalanche photodiodes (APDs) are used in optical receivers of high-speed optical communication systems to improve signal-to-noise ratio over conventional photodiodes. Low excess noise characteristics are crucial for APDs to preserve the benefits associated with high internal gains. In this work, we presented room temperature data of avalanche gain and excess noise factors of Al$_{0.85}$Ga$_{0.15}$As$_{0.56}$Sb$_{0.44}$ APDs using pure and mixed carrier injection profiles. Using pure electron injection, the best possible excess noise performance for a given avalanche width was measured with an excess noise factor < 2 for gains up to 25. This is the lowest excess noise reported for this material system at high gain. Two other injection profiles with increased portion of injected holes worsened the excess noise performance, confirming the need to use pure electron injection for the best possible APD noise performance. The data reported in this article is available from the ORDA digital repository (https://doi.org/10.15131/shef.data.15082455)**

*Index Terms*— **Avalanche photodiodes, impact ionization, excess noise**

## I. INTRODUCTION

Avalanche Photodiodes (APDs) are widely used in optical receivers for high-speed optical fibre-based communication [1] and free-space ranging [2]. Avalanche gain (*M*) from an APD improves the optical receiver's signal-to-noise ratio, provided that the APD's excess noise factor (*F*) and dark current remains low. Therefore, the *F*(*M*) characteristics is one of the key performance parameters for APDs. It is well established that *F* increases with *M* and that the rate of increase is dependent on the material, operating electric field (which leads to a dependence on the avalanche region width), temperature and the carrier injection profile.

To achieve low *F*(*M*) characteristics, it is desirable to use an avalanche material with dissimilar impact ionization coefficients, denoted by *α* for electrons and *β* for holes. Also, it is preferable to inject the carrier type with the larger impact ionization coefficient into the avalanche region to initiate the avalanche multiplication process. Thus, experimental

evaluations of various semiconductor materials and carrier injection profiles have been reported in the literature to identify promising avalanche materials for APDs. APDs designed to detect 1.31 and 1.55 µm wavelengths light adopt a Separate-Absorption-Multiplication (SAM) structure [3]. In a SAM APD, a non-avalanching, narrow bandgap material is used for photon absorption, while a wider bandgap material is used for avalanche multiplication. Typically, In$_{0.53}$Ga$_{0.47}$As or InGaAsP (grown lattice-matched to InP substrates) is used for the former. Hence, research in avalanche materials are often focused on wide bandgap materials that are lattice-matched to InP substrates. They include InP itself [4,5], In$_{0.52}$Al$_{0.48}$As [6], Al$_x$Ga$_{1-x}$As$_y$Sb$_{1-y}$ (with x = 1.0 to 0.80) [7, 8, 9,10], and AlInAsSb [11]. Of these, Al$_{0.85}$Ga$_{0.15}$As$_{0.56}$Sb$_{0.44}$ (referred to as AlGaAsSb hereafter) exhibits lower surface leakage current compared to AlAs$_{0.56}$Sb$_{0.44}$ and excellent *F*(*M*) characteristics, with effective ionization coefficient ratio, $k_{eff}$, as low as 0.05 in APDs with avalanche widths of 87~170 nm [9]. Using mixed carrier injection, $k_{eff}$ ~ 0.01 was recently reported using an AlGaAsSb APD with 1000 nm avalanche width [10]. Since *α* > *β* in AlGaAsSb, using pure electron injection profile is expected to further improve the *F*(*M*) characteristics, reducing $k_{eff}$ value, as any hole injection will adversely increase *F*(*M*). In addition, *F*(*M*) characteristics obtained from pure electron injection can be directly applied for predicting *F*(*M*) characteristics of SAM APDs, which would have pure electron injections into the AlGaAsSb avalanche layer. In this work, we present experimental room temperature (RT) *F*(*M*) characteristics using pure electron injection and a 600 nm AlGaAsSb device *p-i-n* diode. We also present the detrimental effects of mixed injection on *F*(*M*) using two mixed injection profiles.

## II. EXPERIMENTAL DETAILS

The AlGaAsSb p-i-n diode wafer was grown using Molecular Beam Epitaxy on a semi-insulating InP substrate. X-ray diffraction was used to confirm the composition of the AlGaAsSb layers. The wafer structure is summarized in Table 1. The p-, i-, and n- AlGaAsSb layers are sandwiched between

J. Taylor-Mew, V. Shulyak, C.H Tan and J.S. Ng are with the Department of Electronic and Electrical Engineering, The University of Sheffield, Sheffield, S3 JD, U.K. (e-mail: jdtaylor-mew1@sheffield.ac.uk; v.shulyak@sheffield.ac.uk; c.h.tan@sheffield.ac.uk; j.s.ng@sheffield.ac.uk).

B. White, formally with the University of Sheffield, is now with Phlux Technology Limited, North Campus, Broad Lane, Sheffield, S3 7HQ, U.K. (e-mail: ben.white@phluxtechnology.com)

Table 1. Wafer structure

| Material | Doping Type | Doping Density (cm$^{-3}$) | Depth (nm) |
|---|---|---|---|
| In$_{0.53}$Ga$_{0.47}$As | p$^+$ | $2 \times 10^{19}$ | 50 |
| Al$_{0.85}$Ga$_{0.15}$As$_{0.56}$Sb$_{0.44}$ | p | $1 \times 10^{18}$ | 300 |
| Al$_{0.85}$Ga$_{0.15}$As$_{0.56}$Sb$_{0.44}$ | i | - | 600 |
| Al$_{0.85}$Ga$_{0.15}$As$_{0.56}$Sb$_{0.44}$ | n | $1 \times 10^{18}$ | 200 |
| In$_{0.53}$Ga$_{0.47}$As | n$^+$ | $2 \times 10^{19}$ | 500 |
| InP Substrate | | | |

p$^+$-In$_{0.53}$Ga$_{0.47}$As and n$^+$-In$_{0.53}$Ga$_{0.47}$As layers, which facilitate ohmic contacts. Circular mesa devices were fabricated from wafer pieces using standard photolithography and wet chemical etching with two etchants. The first etchant was a solution of Sulfuric acid (H$_2$SO$_4$): Hydrogen peroxide (H$_2$O$_2$): de-ionized water with a ratio of 1:8:80 to remove the top InGaAs layer. This was followed by a solution of Hydrochloric acid (HCl): Hydrogen peroxide (H$_2$O$_2$): di-ionized water with a ratio of 5:1:60 to etch the AlGaAsSb layers. There were four different sizes, with device radius of 210, 110, 60 and 35 µm. Metal contacts were formed by evaporating Ti/Au (20/200nm) on top of the devices (for p-contact) and on the n$^+$-InGaAs layer (for n-contact). The devices were passivated using silicon nitride, before a layer of Ti/Au was deposited as an optical mask. This prevented undesirable injection of incoming illumination to the sides of the devices during avalanche gain and excess noise measurements.

$F(M)$ measurements were carried out at room temperature using a setup reported in [12], which was calibrated with a Si p-i-n photodiode along with the light sources used. The device-under-test (DUT) was illuminated by a continuous-wave light source modulated by a mechanical chopper. This combination produced modulated photocurrent in the DUT, which was under reverse bias, $V$, facilitating phase-sensitive $M(V)$ and $F(M)$ measurements. A transimpedance amplifier converted the modulated photocurrent into modulated voltage, providing
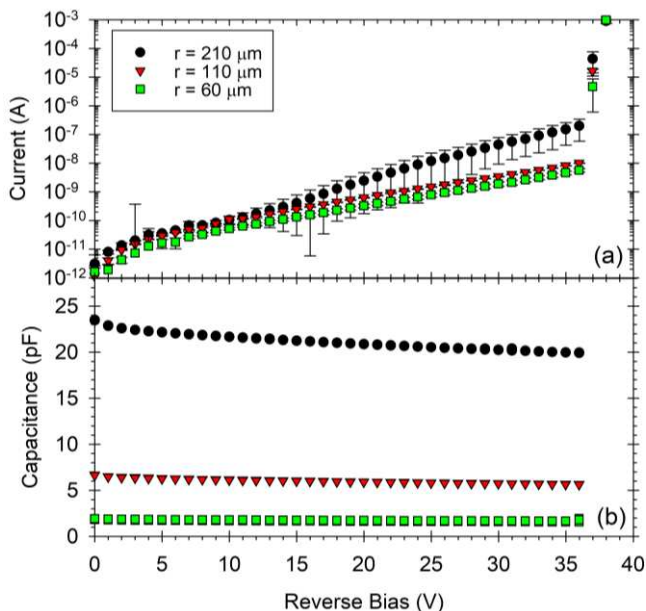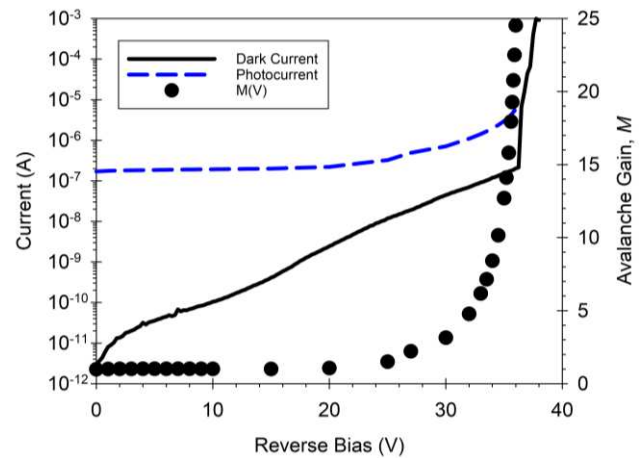


Fig. 2. Example data of dark current and photocurrent (left axis) as well as deduced gain (right axis), obtained from a 210 µm radius device under 420 nm wavelength illumination at room temperature.

avalanche gain data. Small increase in collection efficiency of photo-generated carriers as function of $V$ was taken into account (using linear baseline correction) when extracting $M(V)$. For noise data, the modulated photocurrent went through a bandpass filter (centred at 10 MHz) before being fed to a power meter, producing noise power. The data processing took into account the setup's noise and its dependence on the DUT's capacitance (reference measurement with Si p-i-n diode)

The main $F(M)$ data were obtained using a LED with centre emission wavelength of 420 nm as the light source. This wavelength choice ensured pure electron injection (as in [9]), with > 99.99% of the incoming light absorbed by the point of the p-AlGaAsSb/i-AlGaAsSb junction. The estimate was obtained using Beer-Lambert's Law and absorption coefficients (6.4×10$^5$ cm$^{-1}$ for In$_{0.53}$Ga$_{0.47}$As [13] and 3.0×10$^5$ cm$^{-1}$ for AlGaAsSb [9]). Additional measurements were taken using He-Ne laser emitting at wavelengths of 543 and 633 nm. The percentage of light absorbed by the point of the p-AlGaAsb/i-AlGaAsSb junction is 93.5 and 69.5 %, resulting in mixed carrier injections (ie more holes are injected compared to the pure electron injection condition).



Fig. 1. (a) Mean dark current-voltage data with standard deviations of 210, 110 and 60 µm radii diodes at room temperature. (b) Mean capacitance-voltage for 210, 110 and 60 µm radii diodes.
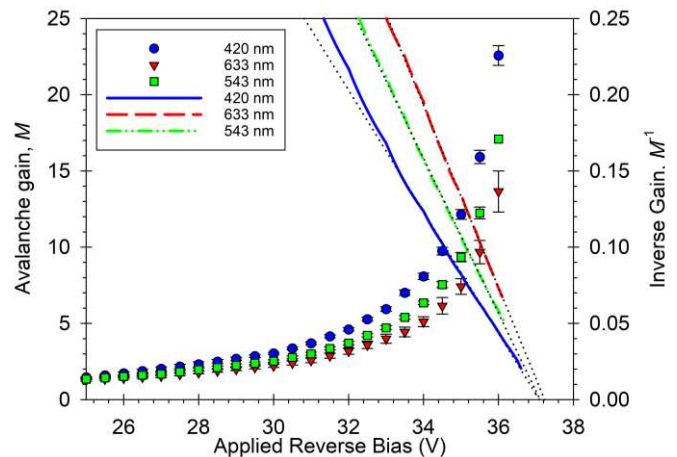


Fig. 3. Avalanche gain versus reverse bias data (mean and standard deviation) obtained using 420, 543 and 633 nm wavelength illumination.
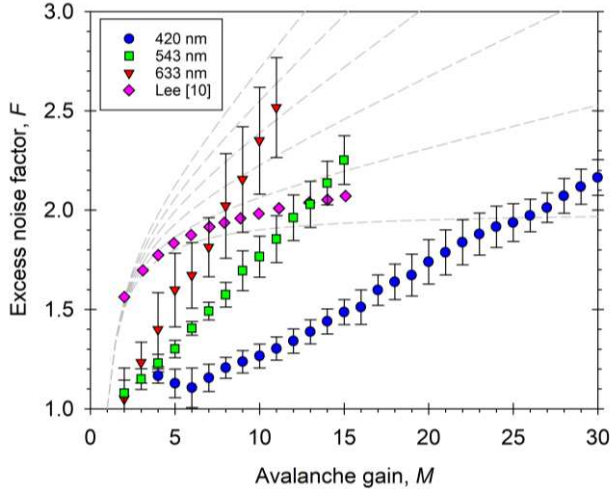
Fig. 4. Excess noise factor versus avalanche gain data (mean and standard deviations) obtained using 420, 543 and 633 nm wavelength illumination. Data from ref [10] (symbol) and McIntyre's local model [16] for fixed $k$ value (0 to 0.1 in step of 0.02, grey lines) are included for comparison.



Fig. 5. Comparison of excess noise factors at avalanche gain of 10 for this work, AlGaAsSb [9,10], AlAsSb [7,14], AlInAsSb [11], InAlAs [6], InP [5] and Si [15].

## III. RESULTS AND DISCUSSION

Reverse dark Current – Voltage characteristics at room temperature were obtained from 4 - 6 devices for each size, the data are presented as mean values and standard deviations in Fig. 1(a). All data exhibit an abrupt increase in dark current at ~ -37 V. Dark current densities from different sized devices (not shown here) disagree, indicating that the surface-related dark current mechanism(s) dominate.

Capacitance – Voltage (C-V) measurements of the different-sized devices are shown in Fig. 1(b). Using 3-region C-V fitting, assuming a constant doping in each of the $p$-, $i$-, and $n$ layers and a dielectric constant of 11.41 [8], we found the i-AlGaAsSb region width was ~608 nm with a background doping of $5 \times 10^{15}$ cm$^{-3}$. C-V data were also used to extract noise power from raw noise measurement data.

Example data of photocurrent and dark current from a 210 µm radius device are shown in Fig. 2. Although the photocurrent is several orders higher than dark current at low biases, the difference reduces as $V$ increases. Hence phase-sensitive measurements are essential in obtaining accurate $M(V)$ and $F(M)$ data. The $M(V)$ and $F(M)$ characteristics at room temperature were obtained from 5 – 15 devices of various sizes.

$M(V)$ data obtained using different wavelengths are compared in Fig. 3. For a given reverse bias, avalanche gain decreases as wavelength increases which is expected as more holes are injected into the avalanche region and $\alpha \gg \beta$ in this material [10]. Data of inverse gain (right axis) confirm avalanche breakdown voltage as -37.2 V.

The corresponding $F(M)$ data are shown in Fig. 4, along with lines of F($M$) based on the McIntyre model [16] for effective k values. Pure electron injection using 420 nm light produced the lowest $F(M)$ data. As wavelength of light increases, there is a monotonic, significant increase in $F$ for a given $M$, indicating the significant impact that carrier injection profile has on the noise performance in AlGaAsSb. This is significant as the $F(M)$ data are lower than those of [10] (a 1000 nm AlGaAsSb pin diode), confirming the need of using pure electron injection for best excess noise performance. Again, this is consistent with
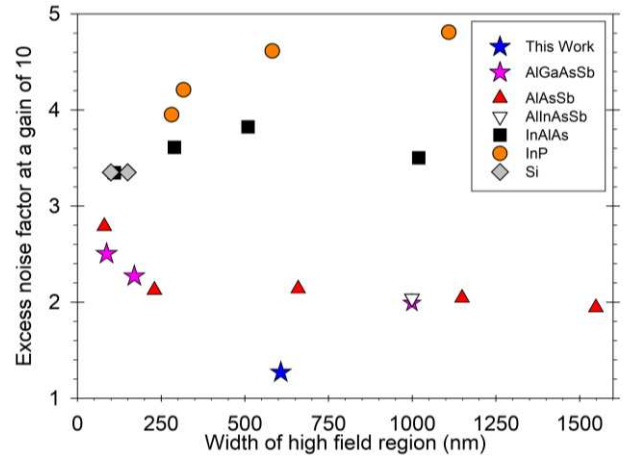
$\alpha \gg \beta$ since excess noise is highly sensitive to changes in carrier injection profile. In Fig. 4, the data set with larger mean F values have larger standard deviations, consistent with the data reported in [9]. This may be due to a combination of greater optical power fluctuation of the light source and/or fewer devices in the data set. In Fig. 4 our data shows $k_{eff} < 0$ for $M <$ 25. This may be due to a combination of $\alpha \gg \beta$ and the effects of carriers' deadspace.

The excess noise factor at $M = 10$ from this work is compared with earlier reports on AlGaAsSb APDs (refs [9] and [10]) in Fig. 5. Other avalanche materials, such as AlAsSb [7, 14], AlInAsSb [11], InAlAs [6], InP [5], and Si [15], are also included. The excess noise performance due to pure electron injection from this work is considerably better than all the other results.

## IV. CONCLUSION

Using a pure electron injection condition, room temperature avalanche gain and excess noise factor were measured on an AlGaAsSb $p$-$i$-$n$ with 600 nm i-region width. At avalanche gains of 10 and 20, the excess noise factors are 1.27 and 1.74, much lower than previous reports on the same material as well as those on relevant avalanche materials. The importance of using pure electron injection is confirmed by degraded excess noise performance when mixed carrier injections (longer wavelengths) were used and demonstrates the potential for a new generation of extremely low noise SAM APDs operating at 1.31 and 1.55 µm wavelengths.

## V. REFERENCES

[1] M. Nada, F. Nakajima, T. Yoshimatsu, Y. Nakanishi, S. Tatsumi, Y. Yamada, K. Sano, and H. Matsuzaki, 'High-speed III-V based avalanche photodiodes for optical communications—the forefront and expanding applications', *Appl. Phys. Lett.*, vol. 116, no. 14, p. 140502, Apr. 2020, doi: 10.1063/5.0003573.

[2] A. M. Pawlikowska, A. Halimi, R. A. Lamb, and G. S. Buller, 'Single-photon three-dimensional imaging at up to 10 kilometers range', *Optics Express*, vol. 25, no. 10, p. 11919, May 2017, doi: 10.1364/OE.25.011919.

[3] S. Xie, X. Zhou, S. Zhang, D. J. Thomson, X. Chen, G. T. Reed, J. S. Ng, and C. H. Tan, 'InGaAs/AlGaAsSb avalanche photodiode with high gain-

bandwidth product', *Opt. Express*, vol. 24, no. 21, p. 24242, Oct. 2016, doi: 10.1364/OE.24.024242.

[4] L. J. J. Tan, J. S. Ng, C. H. Tan, and J. P. R. David, 'Avalanche Noise Characteristics in Submicron InP Diodes', *IEEE Journal of Quantum Electronics*, vol. 44, no. 4, pp. 378–382, Apr. 2008, doi: 10.1109/JQE.2007.914771.

[5] P. Yuan, C. C. Hansing, K. A. Anselm, C. V. Lenox, H. Nie, A. L. Holmes, B. G. Streetman, and J. C. Campbell, 'Impact ionization characteristics of III-V semiconductors for a wide range of multiplication region thicknesses', *IEEE J. Quantum Electron.*, vol. 36, no. 2, pp. 198–204, Feb. 2000, doi: 10.1109/3.823466.

[6] Y. L. Goh, A. R. J. Marshall, D. J. Massey, J. S. Ng, C. H. Tan, M. Hopkinson, J. P. R. David, S. K. Jones, C. C. Button, and S. M. Pinches, 'Excess Avalanche Noise in $In_{0.52}Al_{0.48}As$', *IEEE Journal of Quantum Electronics*, vol. 43, no. 6, pp. 503–507, Jun. 2007, doi: 10.1109/JQE.2007.897900.

[7] X. Yi, S. Xie, B. Liang, L. W. Lim, J. S. Cheong, M. C. Debnath, D. L. Huffaker, C. H. Tan, and J. P. R. David, 'Extremely low excess noise and high sensitivity AlAs0.56Sb0.44 avalanche photodiodes', *Nat. Photonics*, Jul. 2019, doi: 10.1038/s41566-019-0477-4.

[8] X. Zhou, L. L. Pinel, S. J. Dimler, S. Zhang, J. S. Ng, and C. H. Tan, 'Thin $Al_{085}Ga_{015}As_{056}Sb_{044}$ Diodes With Low Excess Noise', *IEEE Journal of Selected Topics in Quantum Electronics*, vol. 24, no. 2, pp. 1–5, 2018. doi: 10.1109/JSTQE.2017.2725441.

[9] L. L. G. Pinel, S. J. Dimler, X. Zhou, S. Abdullah, S. Zhang, C. H. Tan, and J. S. Ng, 'Effects of carrier injection profile on low noise thin $Al_{085}Ga_{015}As_{056}Sb_{044}$ avalanche photodiodes', *Optics Express*, vol. 26, no. 3, p. 3568, Feb. 2018, doi: 10.1364/OE.26.003568.

[10] S. Lee, S. H. Kodati, B. Guo, A. H. Jones, M. Schwartz, M. Winslow, C. H. Grein, T. J. Ronningen, J. C. Campbell, and S. Krishna, 'Low noise $Al_{0.85}Ga_{0.15}As_{0.56}Sb_{0.44}$ avalanche photodiodes on InP substrates', *Appl. Phys. Lett.*, vol. 118, no. 8, p. 081106, Feb. 2021, doi: 10.1063/5.0035571.

[11] S. H. Kodati, S. Lee, B. Guo, A. H. Jones, M. Schwartz, M. Winslow, N. A. Pfiester, C. H. Grein, T. J. Ronningen, J. C. Campbell, and S. Krishna, 'AlInAsSb avalanche photodiodes on InP substrates', *Appl. Phys. Lett.*, vol. 118, no. 9, p. 091101, Mar. 2021, doi: 10.1063/5.0039399.

[12] K. F. Li, 'Avalanche Noise in Submicron GaAs and InP Structures', PhD Thesis, University of Sheffield, 1999.

[13] S. Adachi, 'Optical dispersion relations for GaP, GaAs, GaSb, InP, InAs, InSb, $Al_xGa_{1-x}As$, and $In_{1-x}Ga_xAs_yP_{1-y}$', *Journal of Applied Physics*, vol. 66, no. 12, pp. 6030–6040, Dec. 1989, doi: 10.1063/1.343580.

[14] J. Xie, S. Xie, R. C. Tozer, and C. H. Tan, 'Excess Noise Characteristics of Thin AlAsSb APDs', *IEEE Transactions on Electron Devices*, vol. 59, no. 5, pp. 1475–1479, May 2012, doi: 10.1109/TED.2012.2187211.

[15] C. H. Tan, J. C. Clark, J. P. R. David, G. J. Rees, S. A. Plimmer, R. C. Tozer, D. C. Herbert, D. J. Robbins, W. Y. Leong, and J. Newey, 'Avalanche noise measurement in thin Si p+-i-n+ diodes', *Applied Physics Letters*, vol. 76, no. 26, pp. 3926–3928, 2000, doi: http://dx.doi.org/10.1063/1.126823.

[16] R. J. McIntyre, 'Multiplication noise in uniform avalanche diodes', *IEEE Transactions on Electron Devices*, vol. ED-13, no. 1, pp. 164–168, Jan. 1966, doi: 10.1109/T-ED.1966.15651.